Modal liquid crystal devices in optical tweezing: 3D control and oscillating potential wells

Philip J.W. Hands, Svetlana A. Tatarkova, Andrew K. Kirby, Gordon D. Love

Centre for Advanced Instrumentation, Department of Physics, Durham University, Durham, DH1 3LE, UK
g.d.love@durham.ac.uk

Abstract: We investigate the use of liquid crystal (LC) adaptive optics elements to provide full 3 dimensional particle control in an optical tweezer. These devices are suitable for single controllable traps, and so are less versatile than many of the competing technologies which can be used to control multiple particles. However, they have the advantages of simplicity and light efficiency. Furthermore, compared to binary holographic optical traps they have increased positional accuracy. The transmissive LC devices could be retro-fitted to an existing microscope system. An adaptive modal LC lens is used to vary the z-focal position over a range of up to 100 μm and an adaptive LC beam-steering device is used to deflect the beam (and trapped particle) in the *x-y* plane within an available radius of 10 μm. Furthermore, by modifying the polarisation of the incident light, these LC components also offer the opportunity for the creation of dual optical traps of controllable depth and separation.

© 2006 Optical Society of America

OCIS codes: (230.3720) Liquid-crystal devices; (140.7010) Trapping

---

References and links

1. E.R. Dufresne and D.G. Grier, "Optical tweezer arrays and optical substrates created with diffractive optics," Rev. Sci. Instum. **69**, 1974-1977 (1998)
2. J. Liesener, M. Reicherter, T. Haist and H.J. Tiziani, "Multi-functional optical tweezers using computer-generated holograms," Opt. Commun. **185**, 77-82 (2000)
3. E.R. Dufresne, G.C. Spalding, M.T. Dearing, S.A. Sheets and D.G. Grier, "Computer-generated holographic optical tweezer arrays," Rev. Sci. Instum. **72**, 1810-1816 (2001)
4. J.E. Curtis, B.A. Koss and D.G. Grier, "Dynamic holographic optical tweezers," Opt. Commun. **207**, 169-175 (2002)
5. K. Dholakia, G. Spalding and M. MacDonald, "Optical tweezers: the next generation," Physics World **15**(31), (2002)
6. J.M.R. Fournier, M.M. Burns and J.A. Golovchenko, "Writing diffractive structures by optical trapping," in *Practical Holography IX*, S.A. Benton, Proc. SPIE **2406**, 101-111 (1995)
7. J. Gluckstad and P.C. Mogensen, "Reconfigurable ternary-phase array illuminator based on the generalised phase contrast technique," Opt. Commun. **173**, 169-175 (2000)
8. P.C. Mogensen and J. Gluckstad, "Dynamic array generation and pattern formation for optical tweezers," Opt. Commun. **175**, 75-81 (2000)
9. R.L. Eriksen, P.C. Mogensen and J. Gluckstad, "Multiple-beam optical tweezers generated by the generalized phase-contrast method," Opt. Lett. **27**, 267-269 (2002)
10. P.J. Rodrigo, V.R. Daria and J. Gluckstad, "Real-time three-dimensional optical micromanipiulation of multiple paticles and living cells," Opt. Lett. **29**, 2270-2272 (2004)
11. P.J. Rodrigo, V.R. Daria and J. Gluckstad, "Dynamically reconfigurable optical lattices," Opt. Express **13**, 1384-1394 (2005)
12. M. Kawamura, M. Ye and S. Sato, "Optical trapping and manipulation system using liquid-crystal lens with focussing and deflection properties," Jpn. J. Appl. Phys. **44**, 6098-6100 (2005)
13. M.J. Lang, P.M. Fordyce and S.M. Block, "Combined optical trapping and single-molecule fluororescence," J. Biology **2**, 6 (2003)

14. A. Ashkin and J.M. Dziedzic, "Observation of radiation-pressure trapping of particles by alternating light beams," Phys. Rev. Lett. **54**, 1245-1248 (1984)

15. S.A. Tatarkova, A.E. Carruthers and K. Dholakia, "One-dimensional optically bound arrays of microscopic particles," Phys. Rev. Lett. **89**, 283901 (2002)

16. P.J. Rodrigo, V.R. Daria and J. Gluckstad, "Four-dimensional optical manipulation of colloidal particles," Appl. Phys. Lett. **86,** 074103 (2005)

17. G.D. Love, J.V. Major and A. Purvis, "Liquid crystal prisms for tip-tilt adaptive optics," Opt. Lett. **19**, 1170-1172 (1994)

18. V. Laude and C. Dirson, "Liquid crystal active lens: application to image resolution enhancement," Opt. Commun, **163**, 72-78 (1999)

19. M.A.A. Neil and R. Juskaitis, "Adaptive aberration correction in a two-photon microscope," J. Microsc. **200**, 105-108 (2000)

20. M. Hain, R. Glockner, S. Bhattacharya, D. Dias, S. Stankovic and T. Tschudi, "Fast switching liquid crystal lenses for a dual focus digital versatile disc pickup," Opt. Commun. **188**, 291-299 (2001)

21. M. Ye, B. Wang and S. Sato, "Liquid crystal lens with focus movable in focal plane," Opt. Commun. **259**, 710-722 (2006)

22. A.F. Naumov, M.Y. Loktev, I.R. Guralnik and G.V. Vdovin, "Liquid-crystal adaptive lenses with modal control," Opt. Lett. **23**, 992-994 (1998)

23. A.F. Naumov and G.D. Love, "Control optimisation of spherical modal liquid crystal lenses," Opt. Express **4**, 344-352 (1999)

24. P.J.W. Hands, G.D. Love and A.K. Kirby, "Adaptive modally addressed liquid crystal lenses," in *Liquid Crystals VIII*, I.-C. Khoo, Proc. SPIE **5188**, 136-143 (2004)

25. A.K. Kirby, P.J.W. Hands and G.D. Love, "Optical design of liquid crystal lenses: off-axis modelling," in *Current Developments in Lens Design and Optical Engineering VI*, P.Z. Mouroulis, W.J. Smith and R.B. Johnson, Proc. SPIE **5874**, 07 (2005)

26. A.F. Fray and D. Jones, "Large-angle beam deflector using liquid crystals," Electron. Lett. **11**, 358-359 (1975)

27. D.P. Resler, D.S. Hobbs, R.C. Sharp, L.J. Friedman and T.A. Dorschner, "High efficiency liquid crystal optical phased array beam steering," Opt. Lett. **21**, 689-691 (1996)

28. M. Honma and T. Nose, "Liquid crystal blazed grating with azimuthally distributed liquid crystal directors," Appl. Opt. **43**, 5193-5197 (2004)

29. S. Masuda, S. Takahashi, T. Nose, S. S. and H. Ito, "Liquid-crystal microlens with a beam-steering function," Appl. Opt. **36**, 4772-4778 (1997)

30. T. Nose, Y. Yamada and S. Sato, "Improvement of optical properties and beam steering functions in a liquid crystal microlens with an extra controlling electrode by a planar surface," Jpn. J. Appl. Phys., **39**, 6383-6387 (2000)

31. A.K. Kirby and G.D. Love, "Fast, large and controllable phase modulation using dual frequency liquid crystals," Opt. Express **12**, 1470-1475 (2004)

32. Meadowlark Optics, *www.meadowlark.com*.

33. G. Sinclair, P. Jordan, J. Leach, M.J. Padgett and J. Cooper, "Defining the trapping limits of holographical optical tweezers," J. Mod. Opt. **51**, 409-414 (2004)

34. M. Polin, K. Ladavac, S.-H. Lee, Y. Roichman and D.G. Grier, "Optimized holographic optical traps," Opt. Express **13**, 5831-5845 (2005)

35. C.H.J. Schmitz, J.P. Spatz and J.E. Curtis, "High-precision steering of multiple holographic optical traps," Opt. Express **13**, 8678-8685 (2005)

36. T.-L. Kelly and G.D. Love, "White-light performance of a polarisation-independent liquid-crystal phase modulator," Appl. Opt. **38**, 1986-1989 (1999)

37. G.D. Love, "Liquid crystal phase modulator for unpolarized light," Appl. Opt. **32**, 2222-2223 (1993)

1. Introduction

A number of techniques have been developed to allow the electronic control of optical beams in optical tweezers. These include holographic optical traps (HOTs) [1-6] and the generalised phase contrast (GPC) technique [7-11]. Impressive results have been published using both these techniques showing the manipulation of multiple particles in 3D.

Recently Kawamura *et al*. [12] described results of 3D particle control using a liquid crystal (LC) device with a hole-pattern electrode. In this paper we describe and demonstrate 3D particle manipulation based on modal addressing of LCs, which is a complementary addressing technique. We compare the merits of both these LC technologies with conventional tweezing technologies. Modal LC elements also provide opportunities for controllable dual trap experiments such as individually trapping and stretching long polymer

or protein molecules. We demonstrate the "optical juggling" of a particle between two adjacent potential wells, where the spacing and depths of the well is controllable by the LC.

In general, with LC adaptive elements no complicated alignment procedures are needed, and they are fully electronically controlled (and hence vibration-free). Consequently, we also foresee potential applications of our work in experiments with cold atoms and ions, where crossed focused beams are used to create an interference pattern. Other potential applications include single molecule fluorescence spectroscopy [13], in which combined trapping and spectroscopy can occur, and fluorescence correlation spectroscopy. In the latter example, a combination of single and two-photon correlation spectroscopy is often used; techniques which differ in their sampling volume and depth. LC devices such as those presented here may be able to compensate for this mismatch.

Tweezers using modal LC devices have considerably reduced functionality over a multiple HOT or GPC system, in the sense that in their basic form they can only be used for a single (or double) trap. However, they are considerably simpler, cheaper, and more compact. They also are light efficient and are intrinsically more accurate than a (binary) HOT due to the fact that they are controlled in a fully analogue fashion. In a binary HOT (many published results use ferroelectric spatial light modulators which are binary), the required phase profile to manipulate is binarized and applied to a spatial light modulator along with a carrier frequency. Diffraction means that an array of beams is formed, and one is selected with the appropriate (analogue) phase profile. In our approach we are producing the required phase profiles directly, with little loss of light.

Ashkin and Dziedzic [14] demonstrated optical trapping of a single microscopic particle using radiation pressure of two counter-propagating beams. Since then, counter-propagating beams have been used extensively for the manipulation of cold atoms and ions, and also with larger colloidal particles [15, 16]. In addition to the more conventional technique of optical trapping, the use of our LC devices is also applied to a counter-propagating beams experiment.

Other examples of where similar LC devices have already been successfully implemented include tip-tilt correction in adaptive optics [17], image resolution enhancement [18], aberration correction in multi-photon microscopy [19] and in dual-focus DVD pick-up systems [20].

2. Concept of LC tweezing elements

Two LC-based components are used in addition to the conventional optical trapping equipment, in order to provide additional control and enhance the performance of the system. An adaptive LC lens is used to provide z-axis control, along the direction of the beam, whilst an adaptive LC prism acts as a beam-steering device to provide control in the *x-y* plane. When used together, full x-y-z control of the beam's focal position (and of the optical trap) is achieved. It is also possible to combine both of these functions into a single element [12, 21].

2.1 Concept of operation for LC lens

In a conventional optical tweezing experiment, using an inverted microscope configuration, a microscope objective lens (focal length f_2) is used to focus the incident laser light, thus forming an optical trap for small particles. If an additional lens of focal length f_1 is used in conjunction with the microscope objective, then the change in the incident light's focal position (Δf) is given by Gullstrand's equation:

$$\Delta f = f_2 - \frac{f_1 f_2}{f_1 + f_2 - d} \tag{1}$$

where *d* is the distance between the two lenses. If lens 1 is an adaptive LC lens with electronic control, then clearly the focal length of the system, and hence the position of the optical trap along the z-axis, will also be controllable.

Variable focus lenses are an active area of research, and have wide-ranging applications. A variety of different technologies are used to achieve their goals. In this paper we use a modally addressed LC lens [22-25] in which a quasi-parabolic voltage profile is generated across the aperture of an LC cell of constant thickness, giving rise to a radially symmetric refractive index profile. This is effectively equivalent to a conventional lens of constant refractive index, but with spatially varying thickness. The shape of the voltage profile, and therefore the focussing power of the lens, can be electronically controlled though variation of the frequency and amplitude of the driving voltage. For a full and detailed description of modal lenses, see refs. [22-25].

2.2 Concept of operation for LC beam-steering device

A non-pixellated LC beam-steerer was first proposed by Fray and Jones [26], although its excessive thickness made it extremely slow and impractical for the majority of applications. This paper presents an improvement to that initial design, and implements it into a practical application. In a similar manner to the operation of the modal lens, the LC beam-steering device [17] operates by modifying the voltage profile across an LC cell. The application of a gradient voltage profile (V_1 to V_2) across its aperture gives rise to a gradient in refractive index across the device which can be used to deflect the incoming light through an angle θ given by [17]:

$$\theta = \frac{\Delta n \cdot d}{w}$$
(2)

where Δn is the LC birefringence (0.225 for material E7 at 633nm), *d* is the LC thickness and *w* is the aperture size of the device. For a 50 μm thickness cell with 1 cm aperture, this gives rise to a theoretical maximum deflection angle of 0.0645°. When the beam-steerer is incorporated into the optical trapping experiment, a microscope objective is used to focus the steered beam. At the focal point of the beam, *f*, 17mm away, the maximum steered spot displacement, *s* is therefore given by $f\theta \approx 19.1$ μm. However, for infra-red light at 1064nm, dispersion reduces the liquid crystal's birefringence, limiting the deflection to 1.02×10^{-3} radians (0.0584°). When combined with the aforementioned microscope objective, the available spot displacement is reduced to 17.3 μm.

It is also possible to construct a beam-steerer from pixellated LC-based beam-steering devices including adaptive blazed gratings [27, 28]. Such devices have large steering angles, but suffer from the disadvantage of stepwise approximations and discontinuities in the electric field gradient across the cell. These give rise to undesirable losses through diffraction and scattering. A non-pixellated approach using an LC microlens combined with beam-steering function has also been demonstrated [12, 29, 30]. Its extremely narrow aperture gives rise to a large electric field gradients and a reasonably large deflection range, however additional beam-expanding optics would be required to fill the aperture of the microscope objective of any subsequent trapping system. Then the resulting focus and deflection range will be the same as that produced by the modal approach. The advantage of modal addressing is that it utilizes apertures of arbitrary size, and therefore does not suffer from such limitations. It is also possible to generate other low order wavefront modes, such as spherical aberration [23].

3. Materials and methods

3.1 Optical tweezing arrangement

The experimental set-up is typical for optical tweezing experiments with a single microscope objective in an inverted microscope configuration, used both for focussing the laser light and for observation. We used a ×50, NA=0.42 (MPlan Apo, Mitutoyo) objective lens. A 1W 1064 nm laser beam was expanded to fill the back aperture of the objective and focused onto a ~1 μm spot. This lens is infinity corrected and has a working distance of 17mm. A second objective (suspended above the experiment) was used to illuminate the sample with white light. A hot mirror reflects the laser light into the objective and transmits the white light from a white light source mounted at the top to the CCD camera.

For the counter-propagating beams experiment, the optical set-up is similar to that described in [15]. The laser beam was expanded and split into two intensity equivalent arms, which were then subsequently focused by a pair of identical 50 cm focal length lenses into a rectangular glass cell containing the 2.3 μm particles (Bangs Laboratories, Inc) dispersed in water. The LC prism was introduced into the optical path in an arbitrary position in front of the beam splitter, as no alignment is needed. The observation is carried out with a long-working distance microscope objective (MPlan Apo, Mitutoyo) placed orthogonally to the beam propagation. The particles are observed via the laser light scattered from their surface.

3.2 Construction of the LC devices

As previously described, the lens used in this paper is a modally addressed LC lens [22, 23]. The cell is 50 μm thick with an aperture of 8 mm. The adaptive focussing range is between approximately 90 cm and infinity through the application of voltages in the range 0-20V at 1-5 kHz. Higher focussing power is achievable by the application of higher voltages and frequencies, however aberrations become increasingly more significant beyond this range and a halo of scattered light appears around the focal spot.
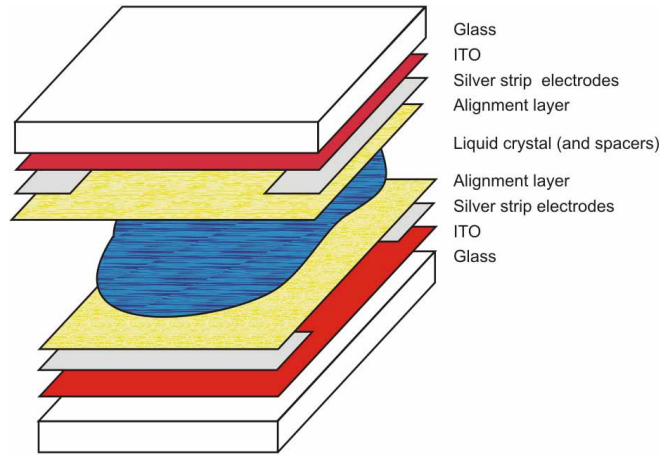
Fig. 1. Construction of the LC beam-steering device

The construction of the liquid-crystal beam-steering device is shown in Fig. 1. ITO-coated glass (Merck) (20 mm x 15 mm x 0.7mm) is sputter coated with silver to form strip electrodes (2 per substrate). A polyimide layer (Merck Liquicoat ZLI-2650) is then deposited by spin-coating, which after baking is rubbed to provide an alignment surface for the liquid crystal. Two substrates are then brought together to form a cell, such that electrodes are inwardly facing and orthogonal to each other (with an offset to expose the underlying

electrodes). Alignment layers are arranged with antiparallel rubbing directions, which is the usual method for producing an LC phase-only modulator (the rubbing of each cell is in opposite directions to give a homogenous cell alignment). The cell is spaced with two 50 μm thickness strips of acetate film, and held together with a UV curable adhesive (Loctite Glass Bond). The empty cell is filled with liquid crystal by capillary action at a temperature above the nematic-isotropic threshold. After cooling, the cell is then sealed with more UV curable adhesive. Connections to the four electrodes are made using adhesive copper tape.

The LC devices described above were designed to have apertures that were an approximate match to the back aperture of the microscope objective. This ensured that when trapping, the full aperture was utilized. However, if one wished to implement similar LC devices to an optical system with a different aperture objective, LC devices of an appropriate size could easily be custom built in order to maximize performance.

4. Results and discussion

4.1 Optical trapping using LC beam-steering device

Before implementation into the optical tweezing experiment, the LC beam-steerer was first tested using a Zygo phase shifting interferometer. The Zygo uses a HeNe laser (633 nm) to map the phase profile across the device whilst it is in operation. Connections to the four electrodes are made as in Fig. 2, giving rise to a linear voltage profile across the cell. For an ideal beam-steering device, a linear gradient in phase shift across the cell is desired. However this cannot easily be achieved due to the non-linear relationship between phase shift and applied voltage for liquid-crystals. To overcome this problem, our driving electronics were designed to operate within the approximately linear region of the phase-voltage relation. For our cell, 5V was found to be approximately in the middle of this linear region. When the cell is in the "off" state (no deflection of beam), $V_1 = V_2 = 5V$ is applied, whilst the lower is grounded. As the beam-steerer is switched "on", the voltages V_1 and V_2 move apart, one increasing from 5V upwards and the other decreasing from 5V downwards, with both voltages still within the region of linear behaviour. As the device is made to steer through increasingly larger deflection angles, the voltages creep further into the regions of non-linearity, resulting in larger optical aberrations. However, if operation is restricted to small deflections and voltages, then linear phase profiles can be maintained with few aberrations.
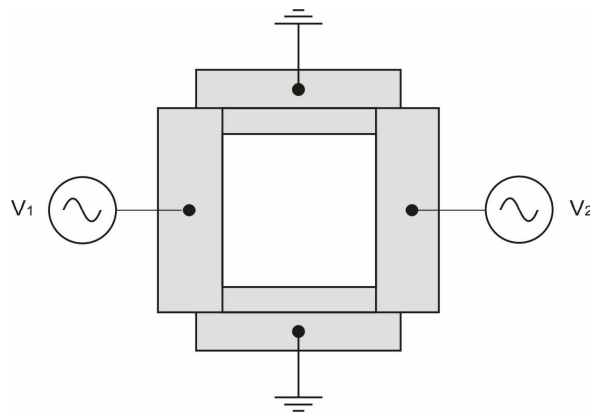
Fig. 2. Electrode connections to the LC beam-steering device

Figure 3 shows how the phase profile across the device varies as a function of voltage across the upper electrode $(V_1 - V_2)$. At $(V_1 - V_2) = 3.75V$, there are approximately 6.5 waves of phase shift across the 1cm aperture, corresponding to 0.024° of steering. This is less than half of the total available steering range achievable with this device. Further increases in the

potential difference were made, resulting in yet steeper phase profile gradients, but the Zygo was unable to resolve fringes of such density, and so the data in Fig. 3 is restricted to voltages lower than 3.75V. Aberrations in the linear phase profile also increase as the potential difference between V_1 and V_2 rises. It is interesting to note that the aberration approximates a weak focus/defocus profile. Future work may possibly involve the use of LC variable lenses to correct for this aberration.
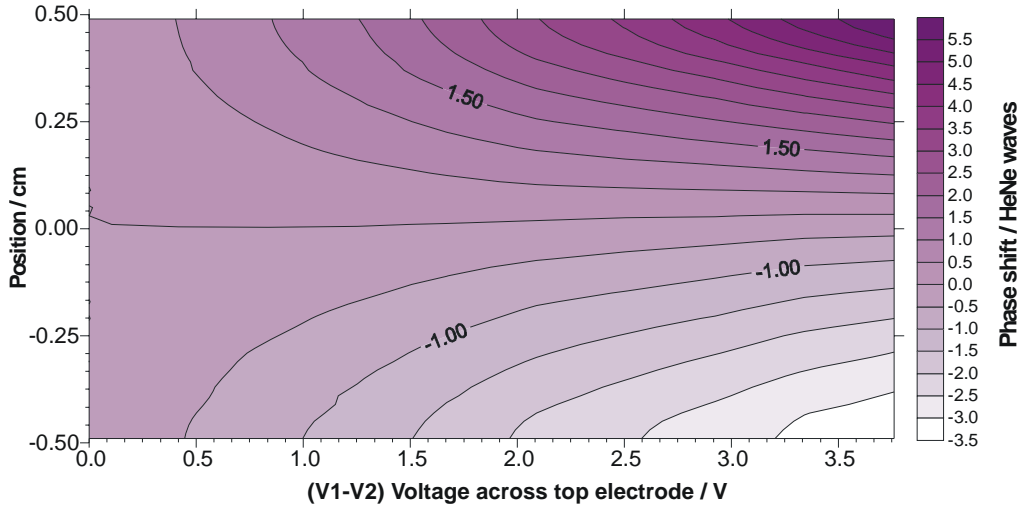
Fig. 3. Contour plot showing phase variation across the LC beam steering device as a function of applied voltage ($V_1 - V_2$).

Further testing of the LC beam-steering device was carried out by passing a polarised, expanded and collimated laser beam (633 nm HeNe) through the LC device, and then using a converging lens (focal length approximately 20 cm) to focus the beam onto a CCD camera. When the device was switched on, controllable deflection in the position of the spot with applied voltage was observed. The separation between the two spots can be controlled by changing the voltage difference ($V_1 - V_2$). Furthermore, by switching the direction of voltages across the cell, the device could be made to deflect the beam in the opposite and also in perpendicular directions. With ($V_1 - V_2$) = 5V, a little less than 200 μm of spot deflection (in each of the four directions) was observed. When compared to the theoretical maximum deflection angle calculated for this system (225 μm), it would appear that approximately 80-90% of the maximum stroke of the device is achievable. Further increases in applied voltage increase the overall phase shift across the device, but at the expense of linearity of the phase profile. The resulting spot then becomes too distorted to view, and would almost certainly be useless as a mechanism for optical trapping.

Next, the device was incorporated into the optical tweezing apparatus. The LC beam-steering device has the advantage that it can be positioned in any location along the collimated beam between the laser and the sample, and re-imaging optics do not need to be used, as is generally the case if mirrors are used.

With incident light polarised parallel to the LC alignment, the focal position of the laser was deflected by the LC device over a controllable range of approximately 10 μm, as shown in Fig. 4. As expected, this distance is slightly less than the calculated theoretical maximum deflection of 17.3 μm, calculated for this particular combination of wavelength, liquid crystal and objective focal length. Once again, only about 80-90% of the full stroke of the LC can be realised, unless the driving voltages are pushed well into the non-linear regions of the LC's

phase-voltage relationship. However, improvements in the overall steering range could be provided through the use of higher birefringence LCs, or by the stacking of multiple devices.
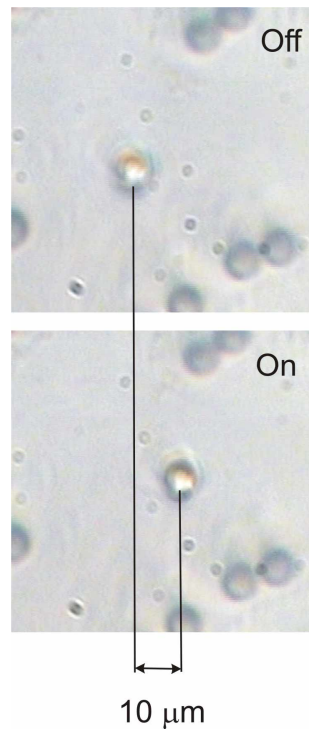
Fig. 4. Deflection of a trapped particle over a 10 µm range using LC beam-steering device.
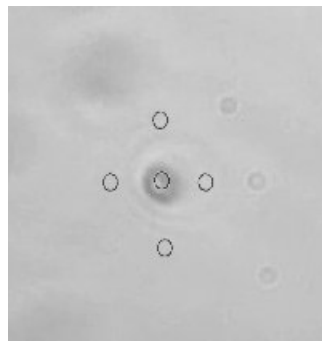
Fig. 5 (video: 2.5 MB). 2x real-time movie of a 3.5 µm trapped particle being moved in the x-y plane by an LC beam-steering device. Circles represent maximum deflection positions. Diameter of total deflection range approximately 20 µm.

When electrode connections to the upper electrode were reversed, 10 µm of movement were also achievable in the opposite direction, giving rise to a total achievable range of approximately 20 µm. Furthermore, movement in the orthogonal directions was also seen after the control electronics were switched appropriately. The result is controllable positioning of the laser focus within the *x-y* plane within a circle of diameter 20 µm (Fig. 5), centred upon the position of the beam when the LC beam-steering device is switched off.

The maximum speed at which trapped particles can be directly steered using the LC beam-steering device is approximately 2 µm/s. This is limited by the switching speed of the liquid crystal. The applied voltage across the beam-steerer can easily be increased more rapidly, but this results in a breakdown in the fringe patterns across the device, which in turn leads to strong aberrations and loss of particle containment. Improvements could be made to this response time through the use of faster switching LC materials [31], or by instead stacking multiple thinner LC devices rather than one thick LC device. Faster particle movement is also possible through the use of dual trap "optical juggling" techniques described in the following section. There is, of course, a maximum speed of motion relating to the strength of the trap.

It is interesting to note that during beam deflection, the position of the trapped particle not only changes within the x-y plane, but also by a small amount in the z-direction. This is because the beam-steering device deflects the focal position of the laser beam along an arc. For small angles, the z-displacement is small, but is just resolvable when the device is switched on at maximum. If displacement is required only in the x-y plane, then a suitable defocus term could be added through use of an adaptive LC lens as described below.

4.2 Dual optical trap experiments using LC devices

It is important to note that light polarised orthogonal to the LC alignment will be virtually uninfluenced by the LC beam-steering device, experiencing a refractive index of n_o and passing undeflected through the cell. Conversely, light polarised parallel to the LC alignment will experience the spatially varying refractive index profile, and will therefore undergo deflection. At intermediate polarisation angles, two spots are visible with different intensities, each representing the component of polarisation either parallel or perpendicular to the LC directors.
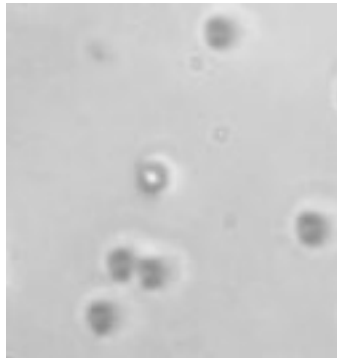
Fig. 6 (video: 1.1 MB). "Optical juggling": Using the LC beam-steering device together with an LC variable retarder, incident polarisation is made to oscillate between states orthogonal and parallel to the rubbing direction. The relative depths (intensities) of the two resulting neighbouring traps is subsequently made to oscillate. A 5 µm trapped particle is therefore repeatedly transferred (juggled) back and forth from one trap to another. (real time)

At an incident angle of 45° to the LC alignment, the two spots have equal intensities. The relative intensities (or trap depths) of the two focussed spots is controllable through variation of the incident polarisation angle. To demonstrate this, a liquid crystal variable retarder (Meadowlark Optics [32]) was combined with the optical tweezer set-up. The variable retarder was located in the beam in front of the beam-steering device, and was programmed (with a square wave) to oscillate between parallel and orthogonal polarisation angles (relative to the LC beam-steerer's rubbing direction). The two neighbouring trapping sites, formed from the two orthogonal states of polarisation, are therefore switched on and off sequentially

in a binary fashion. The result was that a 5 μm trapped particle could be transferred back and forth from one trap to the other in a form of "optical juggling" (Fig. 6). This type of particle transfer could be successfully performed over the full range of displacements achievable by the LC beam-steering device. However, the speed at which this transfer can occur is much more rapid than that achievable by direct beam-steering.

4.3 Optical trapping using LC lens

(a)

Lens slowly switched on, trapped particle being moved out of focal plane

Camera refocussed   Lens switched off   Camera refocussed

(b)

Trapped particle in focus

(c)
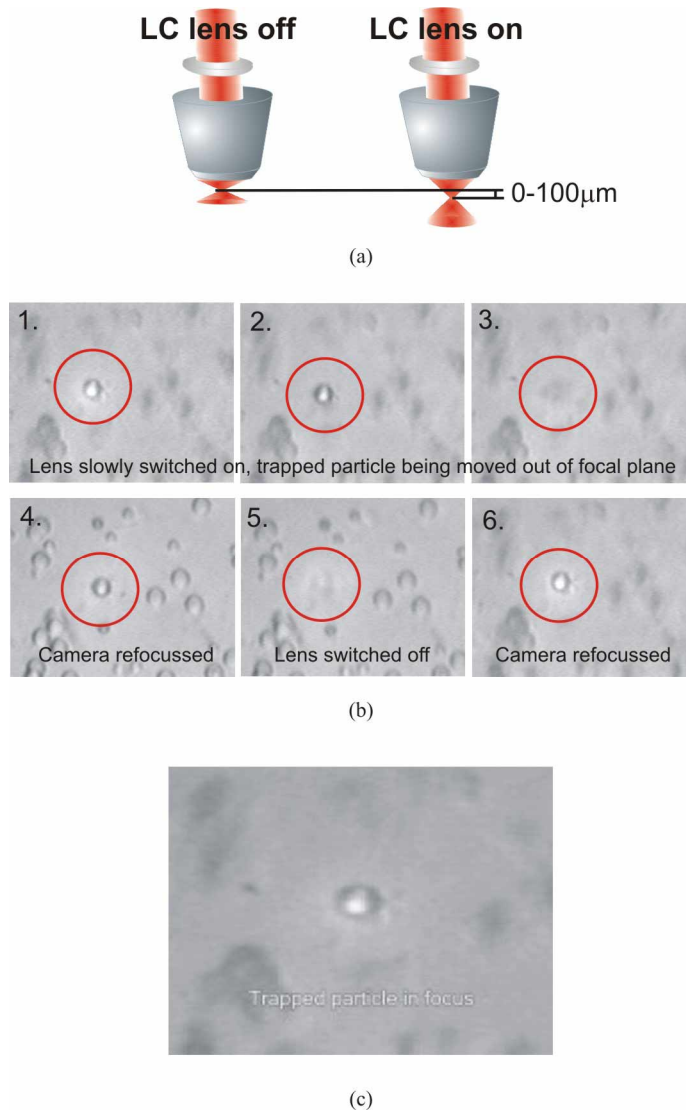
Fig. 7. Z-axis control of optical trapping using a modal LC lens. (a) Greater than 100 μm of focus variation are achievable with the device. (b) Sequence of images showing how a trapped particle can be moved along the z-axis, in and out of the plane of camera focus. In (1) the trapped particle is in a different vertical plane to most of the other particles (which are stuck to the cover glass. In (2)-(3) the trapped particle is moved in the z-direction – and so its image is defocused. In (4) the camera was refocused on the new particle position. In (5) the lens is switched off and the particle moves back to its original trapped position as shown in (6) and the camera is re-focussed. (c) (video: 2.2 MB) Video of z-axis movement control (3x real-time).

The LC lens was implemented into the path of a conventional laser trapping experiment, in front of the microscope objective. The losses due to the insertion of the lens were <10%.

Manipulation of a particle's vertical position was be achieved at submicron accuracy, over a range of over 100 μm, which was only limited by the depth of the sample cell itself. From equation 1, it follows that for our system, with the LC lens 5 cm away from the back aperture of the microscope objective, the achievable range of z-axis movement, given by Δf, would be 1 mm. A demonstration can be seen in Fig. 7. The lens is switched on, causing the particle to move increasingly further out of the plane of observation over a range of approximately 100 μm. The camera is then adjusted so that the particle is refocused at its new position.

Once again, the birefringent nature of the LC lens gives rise to the potential of generating dual traps with orthogonal polarisation. By aligning the polarisation of the incident beam to some angle between 0 and 90° to the LC alignment, it was possible to simultaneously generate two independent optical traps which were stacked above each other in the z-direction. By varying the voltage and frequency supplied to the lens, and hence its focal length, the separation between the two traps could be controlled up to a maximum of 100 μm.

Improvements to the dynamic range of the LC lens can be made in a number of different ways. In a similar manner to the LC beam-steering device, use of higher birefringence LCs, the use of thicker cells or the stacking of multiple lenses will increase the available stroke of the device. Alternatively, the aperture of the LC lens can be reduced, giving rise to a more powerful lens with shorter minimum focal length.

Furthermore, by adjusting the angle of polarisation of the incident light with an LC variable retarder, the relative intensities of the two emerging beams (and hence the relative depths of the two vertically stacked optical traps) are also able to be controlled. "Optical juggling" experiments along the z-axis direction are therefore also entirely feasible.

4.4 Single optical trap formed by counter-propagating beams
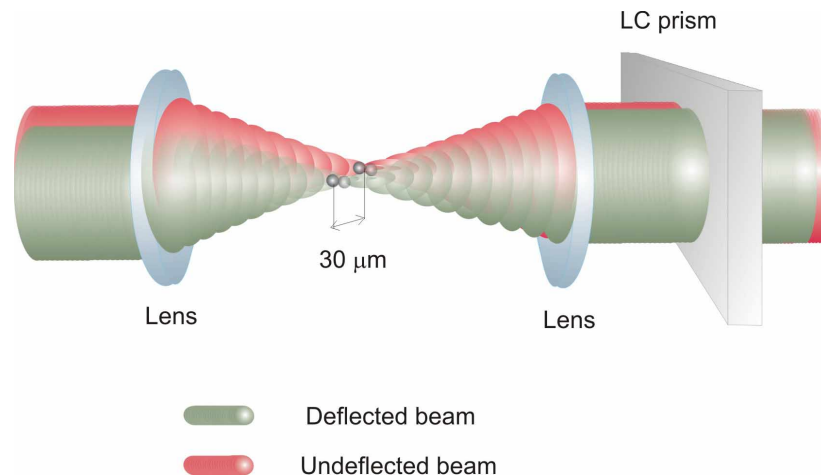
Fig. 8. Diagram showing how deflection of one of the beams within a counter-propagating beams optical trap gives rise to approximately 30 μm of deflection along the beams' axes. A small and less significant vertical deflection of approximately 2 μm also occurs.

With the LC alignment in the beam-steering device aligned parallel to the laser polarisation, a single set of counter-propagating beams is observed. The particle is stable and almost motionless (except for random diffusion kicks) at the bottom of the potential well formed by the two focused beams. The LC beam-steering device was switched on, introducing a small

tilt between the two beams and moving the equilibrium position of the particle. The LC device response time is between 1 and 3s. In comparison, the relaxation of the particle at the bottom of potential well occurs at approximately 300 Hz - faster then the LC switching time. Therefore the stability of the particle is unaffected by the use of such LC elements.

(a)   (b)
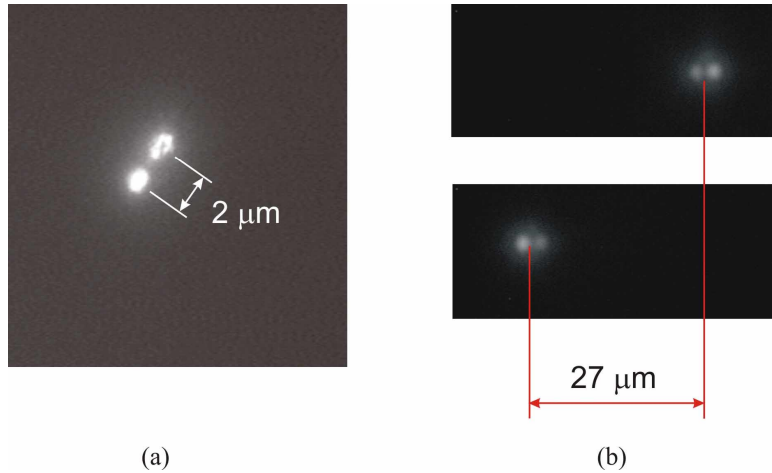
Fig. 9. Movement of two particles held within a single trap formed from two counter-propagating beams combined with an LC beam-steering device. As the beams are deflected, 2 μm of transverse deflection are observed (a), whilst 27 μm of movement is achieved in a direction parallel to the beams' axes (b).
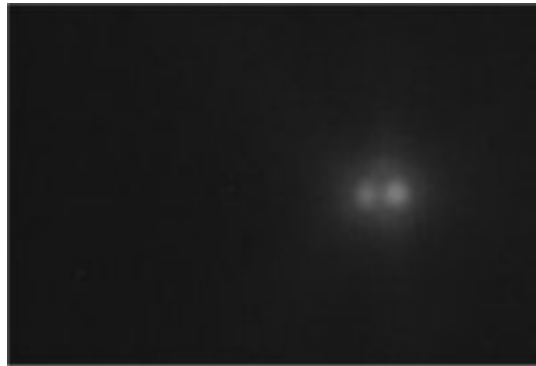
Fig. 10 (video: 2.5 MB). Movie of particles being moved over a 27 μm range by an LC beam-steering device controlling a trap formed by two counter-propagating beams. (2x real-time)

The motion of two 2.3 μm particles, trapped together in a single trap formed by the two counter-propagating beams was observed. When the prism was switched partially on (ie: $(V_1 - V_2) = 3.75V$), the particles moved 2 μm in the direction of applied voltage and along the beam's axis by 27 μm (Fig. 9 and 10). This is concurrent with the movement of the intersection position of the two focussed beams (Fig. 8). Larger movements should also be possible, with further increases in the driving voltages. By varying the control voltage, intermediate positioning was also possible up to an accuracy of 0.5 μm. The movie in Fig. 10 shows the average speed of displacement along the beam's axis from one equilibrium position to another is approximately 2-3 μm/s if the prism is suddenly switched on (note video speed is 2x real-time), although it can be moved more slowly if desired by ramping the voltage across

the beam-steering device more slowly. These changes do not affect the stability of the particle in the trap and do not bias with the step-wise motion of conventional motorized stages normally employed for such experiments.

5. Positional accuracy of optical traps.

The accuracy of optical traps has been considered in refs [33-35]. Sinclair *et al.* [33] considered the efficiency of the trap versus displacements. Both Polin *et al.* [34] and Schmitz *et al.* [35] showed that the positional accuracy of a HOT is related to both the number of pixels and the number of phase levels. For a typical SLM with grey-scale capability, sub-nano meter positional accuracy can be achieved. Many of the commercially available devices use binary ferroelectric LCs in which case the accuracy will be reduced. Even for grey-scale SLMs, when the number of trapping sites is increased then the positional accuracy will decrease. The prisms and lenses described in this paper are truly analogue devices, and thus, in principle, can be controlled to an arbitrary accuracy. In practice the limit will be given by the thermal stability (which can be controlled) and the stability of the control electronics. It may be useful to combine a HOT with an LC lens or prism so, for example, full 2D control of the particles can be achieved with a HOT in combination with an LC lens to control the z-direction, assuming all the particles move in the same sense. Obviously there is a trade of increased simplicity and accuracy in the 2D control at the expense of having all the particles move in the z-direction simultaneously.

6. Conclusions

Electronic variable positional control of an optical tweezing trapping site is demonstrated in three dimensions. An adaptive modal LC lens is used to provide adjustment of the focal length of the system, giving a controllable range of over 100 μm in the z-direction. Movement in the *x-y* plane is provided by an LC beam-steering device, which operates as an adaptive prism, offering a steerable range for a single spot of approximately 20 μm. Further enhancements to this adaptive range should also possible through the use of higher birefringence LCs, by the use of cells of greater thickness and by the stacking of multiple devices. Additionally, the choice of microscope objective used in the tweezing apparatus will determine the exact amount of controllable deflection. The control of unpolarised laser light it also possible by replacing each LC device with two orthogonal devices or by using the double pass technique described in references [36, 37].

The use of LC elements in optical trapping also offers the unique opportunity to easily generate dual trapping sites with variable separation in any of the *x*, *y* or *z* directions. This offers the opportunity for a large number of experiments that involve the manipulation (stretching, compressing) of long molecules; experiments that would otherwise require the use of highly expensive and sophisticated SLM control. Additionally, by controlling the polarisation of the incident laser beam with an LC variable retarder, the relative depths of the two traps are adjustable. An "optical juggling" experiment is demonstrated to illustrate this, whereby particles are repeatedly transferred back and forth from one optical trap to another. This type of positional control offers more rapid movement of trapped particles (over the same range) compared to direct LC beam-steering alone.

The application of LC beam-steering devices in counter-propagating beam trapping experiments has also been demonstrated. With the device partially (~20%) switched on, 27 μm of controllable movement along the beams' axes is observable.

Acknowledgments